Electronic Structure of Metal-Free Porphyrazines in Thin Films

D. Pop,*,† B. Winter,† W. Freyer,† I. V. Hertel,† and W. Widdra†,‡

Max-Born-Institut für Nichtlineare Optik und Kurzzeitspektroskopie, Max-Born-Strasse 2A, D-12489 Berlin, Germany, and Institut für Atomare Physik und Fachdidaktik, Technische Universität Berlin, D-10623 Berlin, Germany

Received: May 23, 2003; In Final Form: August 14, 2003

We report photoemission spectra of the valence region for a series of linearly benzo-annelated porphyrazine molecules in thin films. This family of compounds, with stepwise varied ligand size, is an ideal model system to investigate the evolution of the electronic structure with the increasing π-electron system of the molecule. Specifically, the electronic structure of *tert*-butyl-substituted metal-free tetraazaporphyrin, phthalocyanine, and naphthalocyanine is investigated by photoelectron spectroscopy using synchrotron radiation in the 70−105 eV photon energy range. A shift of the highest occupied molecular orbital toward lower binding energies as a function of the increasing ligand size is found and discussed on the basis of existing theoretical calculation. Only a small influence of the *tert*-butyl substituent group on the photoemission spectra is observed as compared to spectra of unsubstituted molecules.

1. Introduction

The family of porphyrazine molecules has attracted much interest due to both the potential in technological applications and their close relationship to the biologically important porphyrins, such as chlorophyll and hemoglobin molecules. The remarkable construction of porphyrazines, characterized by high symmetry, planarity, and electron delocalization made these molecules also a challenge for theoretical studies.

Porphyrazines contain a central conjugated C_8N_8 ring with four pyrrole groups (see Figure 1). The analogies between porphyrazines and porphyrins are based on their similar chemical structure; they only differ by the presence of four meso-nitrogen atoms (in porphyrazines) as opposed to four methine groups (in porphyrins) in the central ring. The class of porphyrazine molecules is generally understood to include the tetraazaporphyrin (TAP or porphyrazine) and its analogues: the phthalocyanine (Pc), naphthalocyanine (Nc), and anthracyanine (Ac) molecules.

The chemical versatility of the porphyrazine macrocycle offers the opportunity of varying the electronic structure through modifications of the ligand and the central atoms (two hydrogen atoms in Figure 1, but often also a metal atom). Substitutions to the macrocycle by electron-withdrawing or electron-donating groups were found to considerably change the electronic properties.[1−3] Another way to adjust the molecular properties is to modify the extension of the π-electron system. Several studies were concerned with extended porphyrazine compounds that have additional aromatic rings attached to the skeleton of the porphyrazine molecule.[3,4]

The wide interest for these molecules,[4−11] ranging from biology to technological applications, clearly demands a detailed understanding of their electronic structure. A suitable technique by which this information may be accessed is photoelectron spectroscopy. The present paper focuses on the photoemission in the valence region from thin films of porphyrazine molecules with stepwise extended π-electron systems. This ligand variation is done by systematically increasing the number of benzo units through linear benzo annelation. Thus, the series of investigated compounds consists of molecules containing 0, 4, and 8 benzo units. Photoemission spectra, in this photon energy range, from metal-free tetraazaporphyrins have not been previously reported. Therefore, together with recent theoretical work[12−17] the present results contribute to a better understanding of the electronic structure of tetraazaporphyrin compounds. We present also for the first time the photoemission spectra of thin films of *tert*-butyl-substituted metal-free phthalocyanine and naphthalocyanine.

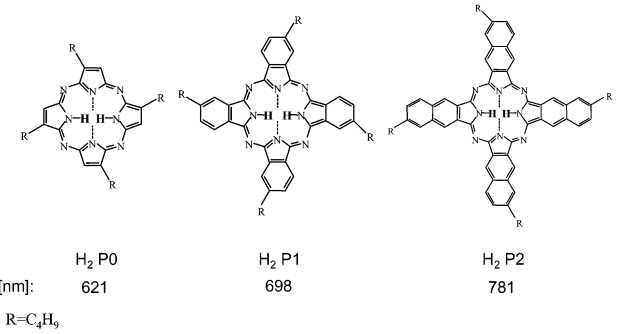

Figure 1. Illustration of the molecules investigated in the present work. R denotes a *tert*-butyl group. The absorption wavelengths of the Q_x component of the Q-band (compounds dissolved in benzene) are given (see Figure 2). These values have ±1 nm uncertainty.

2. Experimental Section

2.1. Materials and Thin Film Preparation. The porphyrazine molecules investigated in the present work are sketched in Figure 1. The chemical names of the molecules, from left to right in Figure 1 are tetra(*tert*-butyl)porphyrazine, tetra(*tert*-butylbenzo)porphyrazine (or tetra(*tert*-butyl)phthalocyanine), and tetra(*tert*-butylnaphtho)porphyrazine (or tetra(*tert*-butyl)-naphthalocyanine), respectively. Throughout the paper these molecules will be referred to as H_2P0, H_2P1, and H_2P2, where

† Max-Born-Institut für Nichtlineare Optik und Kurzzeitspektroskopie.
‡ Technische Universität Berlin.

10.1021/jp030647g CCC: $25.00
Published on Web 09/27/2003

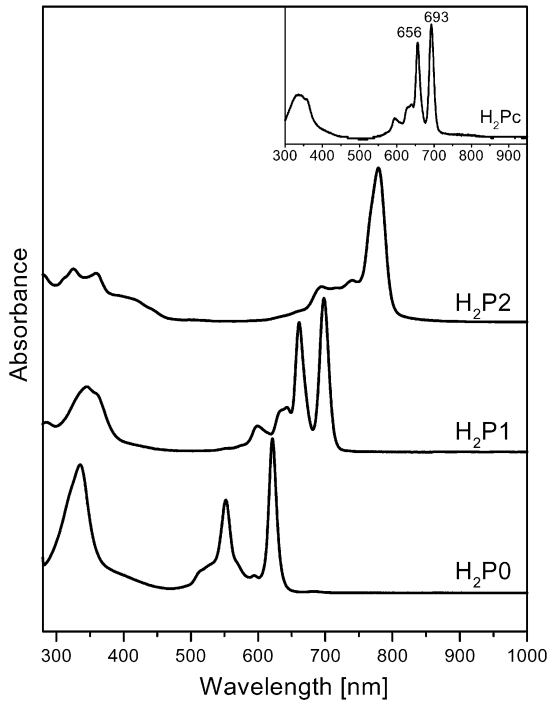

Figure 2. Optical absorption spectra of H_2P0, H_2P1, and H_2P2 dissolved in benzene. For reference, the inset shows the optical absorption spectrum of H_2Pc.

the numbers 0, 1, and 2 represent the number of benzo units fused to each pyrrole group. Note that the molecules in Figure 1, in the absence of any *tert*-butyl substituent (denoted by R) would correspond to metal-free tetraazaporphyrin (or metal-free porphyrazine) (H_2TAP), phthalocyanine (H_2Pc), and naphthalocyanine (H_2Nc), respectively. *tert*-butyl substitution facilitates the synthesis of the molecules in solution. All molecules were synthesized and characterized at the Max-Born-Institut. H_2P1[18] and H_2P2[19] were prepared by modified standard methods.[20,21] The preparation of H_2P0 was done via the magnesium complex;[22] however, in certain cases we also used the commercial product from Aldrich. The compounds were purified and characterized by thin-layer chromatography, HPLC, high-vacuum sublimation, absorption and fluorescence spectroscopy, and mass spectrometry. The purity of the materials, estimated by fluorescence spectroscopy, was better than 99.9%.

Optical absorption spectroscopy was also performed for characterizing the compounds under investigation. The absorption spectra of the compounds dissolved in benzene are shown in Figure 2. *tert*-Butyl substitution only insignificantly alters these spectra. As shown in the inset, just a small shift of the first absorption maximum (from 693 to 698 nm) is observed for H_2Pc upon *tert*-butyl substitution. However, the increase in the number of benzo units causes a dramatic shift of the Q-band absorption maximum toward larger wavelengths, which is indicative of a wider delocalization of the molecular π-electron system.[23−25] In contrast to metal-containing porphyrazines that have D_{4h} symmetry, the metal-free porphyrazines exhibit a splitting of the Q-band due to the reduced D_{2h} symmetry, which removes the degeneracy of the lowest unoccupied molecular orbital (LUMO).[26] This splitting is best seen for the H_2P0 and H_2P1 films in the 530 to 650 and 650 to 730 nm range, respectively. For H_2P2 it leads to a broadening of the absorption peak at 781 nm.

The organic films were deposited by sublimation on a Au(111) single crystal in ultrahigh vacuum (2×10^{-10} mbar base pressure). The material was evaporated from open quartz crucibles mounted at approximately 5 cm distance from the 10 mm diameter gold sample. During deposition the crystal was kept at room temperature. Prior to the deposition the gold substrate was cleaned by repeated cycles of Ar^+ sputtering and annealing to 750 °C.

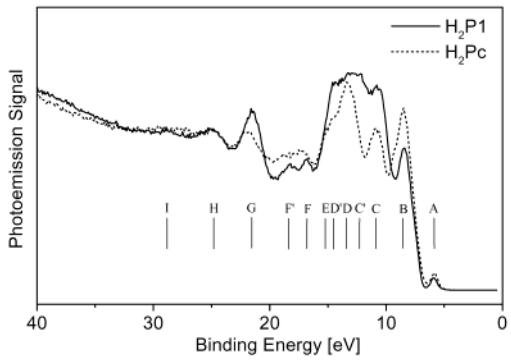

Figure 3. Photoemission spectra from unsubstituted H_2Pc (dashed) and H_2P1 (solid) thin films for 90.6 eV photon energy. Electron binding energies are given with respect to the vacuum level. Intensities are normalized to the signal intensity found at 32 eV binding energy.

The Au(111) single crystal was mounted on a manipulator, which allowed for sample rotation (azimuth Φ, tilt Ψ, polar Θ) and translation (x, y, z) in front of the energy analyzer. All experiments were conducted at room temperature.

The sublimation temperatures for film preparation were 180, 350, and 500 °C for H_2P0, H_2P1, and H_2P2, respectively. As the largest molecule, H_2P2, is susceptible to a slow fragmentation at elevated temperatures, its deposition time was kept below 20 min. For H_2Pc the deposition temperature was 380 °C. The optical absorption spectra of a native material (in solution) and that recovered by dissolving the material from a quartz plate on which the respective film was grown under the actual preparation conditions did not show any difference. Therefore, it was inferred that the films contained only intact molecules.

In the case of H_2Pc, the typical film thickness was estimated to be about 400 ± 40 Å. This was determined from the deposition rate monitored by a quartz crystal microbalance. The H_2P0, H_2P1, and H_2P2 films were prepared to have the same number of molecules, on the basis of the monitored film thickness and the molecular mass. After film preparation the sample was transferred into the analysis chamber for photoemission measurements under ultrahigh-vacuum conditions.

2.2. Photoelectron Spectroscopy. The photoemission experiments were performed at the MBI-BESSY beamline at the synchrotron radiation facility BESSY. This beamline provides photon energies from 20 to 180 eV using a monochromator that has two rotatable spherical gratings in combination with an adjustable planar mirror (VIA principle).[27] The energy resolution for 64 eV photons is about $E/dE = 6000$ at ca. 4×10^{12} 1/(s 100 mA) photon flux. The analysis chamber (base pressure better than 2×10^{-10} mbar) is equipped with a hemispherical electron energy analyzer EA 125, Omicron. Photoelectrons were detected at 1° acceptance angle. The energy resolution of the spectrometer was typically 150 meV using 10 eV pass energy. The photoelectrons were detected in normal emission geometry with grazing light incidence (83° with respect to the surface normal).

3. Results and Discussions

Effect of the *tert*-Butyl Substituent on the Photoemission Spectra. Figure 3 shows a comparison of photoemission spectra of thin films of H_2P1 (solid line) and unsubstituted H_2Pc (dashed

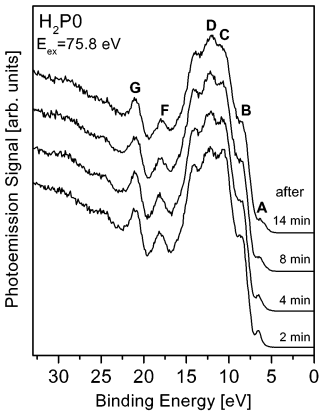

Figure 4. Photoemission spectra of a H_2P0 thin film as a function of synchrotron radiation exposure, measured on an identical surface spot. The respective exposure times are indicated, and the spectra are vertically displaced for clarity.

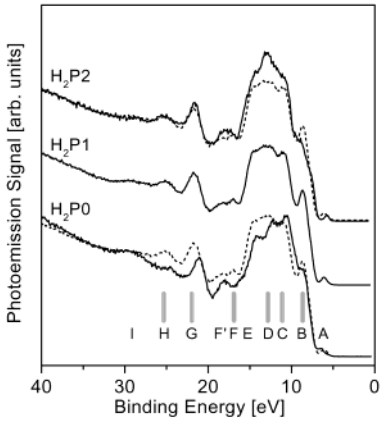

Figure 5. Photoemission spectra of H_2P0, H_2P1, and H_2P2 thin films obtained for 93.7 eV photon energy. Electron binding energies are given with respect to the vacuum level. The dashed spectrum overlapped on the H_2P0 spectrum and on the H_2P2 spectrum is the spectrum of H_2P1 compound (center panel). The shaded bars identify features containing benzene contributions.

line) for an excitation energy of 90.6 eV. The spectra are normalized to the signal intensity found at 32 eV binding energy. Except for the additional features C′ and D′ we use the peak notation introduced by Orti and Bredas for H_2Pc.[28] Following their assignment, peak A is derived from C2p π orbitals that form the highest occupied molecular orbital (HOMO), whereas feature B contains benzene π and nitrogen contributions, C includes benzene σ, π and pyrrole aza nitrogen contributions, D, F, G, and H contain emission from benzene, feature E is attributed to 2p contributions from carbon and nitrogen atoms in the central molecular ring, F′ includes the signal from C2s orbitals in the central molecular ring, and I originates from the emission of the N2s orbitals of the nitrogen atoms within the pyrrole groups. Although the HOMO for H_2Pc spreads over the carbon backbone, the main contribution arises from the carbon atoms forming the inner carbon−nitrogen ring. Conversely, the HOMO−1 is largely localized on the nitrogen atoms.[14]

Binding energies are similar for H_2Pc and H_2P1 films. The effects of the four *tert*-butyl groups are an increase of the intensity and a slight shift of feature G as well as additional contributions in the 9.5−16 eV binding energy range. The position of the HOMO (feature A) is unshifted upon *tert*-butyl substitution. Notice that in the optical absorption spectrum too, only a small shift of the Q_x band is observed upon *tert*-butyl substitution. The apparent intensity decrease of feature B in H_2P1, as compared to H_2Pc, is largely due to the normalization (at 32 eV), which reduces its relative intensity for the larger (substituted) molecule. Overall, the differences between the photoemission spectra of substituted and unsubstituted compounds are mainly the additional contributions originating from the *tert*-butyl groups. Similar effects are expected to appear also at the *tert*-butyl substitution of the other metal-free porphyrazines.

Photostability. The effect of synchrotron radiation exposure on the photoemission spectra has been investigated, because possible photodegradation needs to be taken into account for a meaningful analysis of the data. As an example, in Figure 4 we illustrate the photostability of a H_2P0 film, which is the most sensitive one studied here. The figure depicts photoemission spectra for subsequent synchrotron radiation exposure at 75.8 eV photon energy. The observed spectral changes are most pronounced for the HOMO, which shows a substantial peak broadening. Considerable peak broadening is also observed for features B, C, and to lesser extent also for features G and F. The nature of these changes has not been investigated here. Synchrotron light-induced changes in the H_2P1 films are considerably weaker and have only been seen for much longer exposure times. The H_2P2 film is the most stable one. Hence, it seems that the central porphyrazine ring is the most sensitive molecular unit to VUV irradiation. Apparently, the addition of benzo units enhances the overall photostability. For the present photoemission experiments the surface spots were frequently changed to minimize the radiation-induced effects.

Ligand Size Dependence. Photoemission spectra of thin H_2P0, H_2P1, and H_2P2 films obtained for 93.7 eV photon energy and normalized to the signal intensity found at 32 eV are displayed in Figure 5. For better comparison the H_2P1 spectrum has been plotted (dashed line) on top of the H_2P0 and H_2P2 spectra. Note that the H_2P0 spectrum (Figure 5 bottom) is the first photoemission spectrum of the valence region reported for a metal-free tetraazaporphyrin. The assignment of the photoemission features in the H_2P0 spectrum follows directly the H_2P1 assignment, which in turn is based on H_2Pc: the contributions arising from the additional benzene units and also from the substituent can be well distinguished. Because the phthalocyanine photoemission spectrum may be regarded as being composed of four benzene rings and a central carbon−nitrogen ring,[28,29] the features of increased relative intensities for the H_2P1 compound are directly attributed to benzene contributions. These positions are indicated by labels (shaded bars) in Figure 5. The majority of the photoemission features for H_2P0 is shifted to lower binding energies with respect to those of H_2P1, by about 0.4 to 0.8 eV. Peak F′ stays at fixed energy for the two compounds, most probably because it originates from the carbon atoms within the central ring of the molecule. The HOMO in H_2P0 (feature A) is found at larger binding energy relative to the H_2P1 case. The apparent higher intensity of feature C in H_2P0 as compared to H_2P1 is attributed to an increased background in the latter case.

The assignment of the H_2P2 spectra may be inferred by an analogous comparison with H_2P1. Except for feature B, peaks attributed to orbitals of benzene constituents increase in intensity, and except for the HOMO/band A, no significant peak shifts are observed. Bands F and F′ are no longer resolved and form a broad feature. The intensity decrease of feature B relative to that in H_2P1 is attributed to a peak broadening and shift toward higher binding energy (see also Figure 6). The electronic structure of unsubstituted naphthalocyanine can be regarded as being formed by adding four naphthalene moieties to the central carbon−nitrogen ring.[30,31] Hence, the peak assignment can be

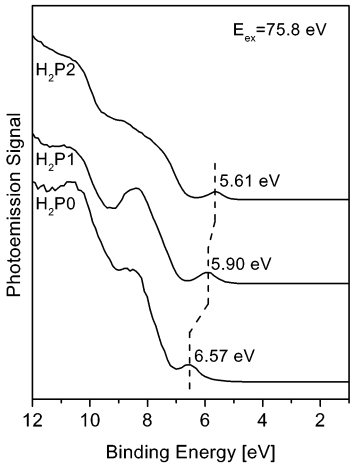

Figure 6. Photoemission spectra for thin films of H_2P0, H_2P1, and H_2P2 in the HOMO region. Labels mark the respective HOMO binding energies. The error bars for the binding energies are ±0.07 eV.

TABLE 1: Experimentally Determined Binding Energies for the HOMO, the First Absorption Maximum (E_{abs}) for the Compounds Dissolved in Benzene, and Estimated LUMO Binding Energies (Approximated by $E_{HOMO} - E_{abs} = E_{LUMO}$)[a]

compound	HOMO[b] (eV)	first abs max. (benzene soln) (eV)[b]	LUMO[c] (eV)	calc HOMO[d] (eV)	calc LUMO[d] (eV)
H_2P0	6.57 ± 0.07	2	4.57	7.3	5.22
H_2P1	5.9 ± 0.07	1.78	4.12	6.42	4.61
H_2P2	5.61 ± 0.07	1.59	4.02	6.05	4.4

[a] For comparison, calculated binding energies for the HOMO and the LUMO of compounds without *tert*-butyl substitution[14] are also given. [b] Present study. [c] Assuming for simplicity $E_{LUMO} = E_{HOMO} - E_{abs}$. [d] Calculated for the corresponding unsubstituted compounds.[14]

based on refs 14, 28, and 30: Band A at 5.61 eV binding energy is attributed to the HOMO. Its orbital character is similar to the HOMO of H_2Pc. Band B contains contributions from π molecular orbitals in naphthalene and also from nitrogen atoms, whereas band C includes σ and π molecular orbital contributions as well as emission from nitrogen atoms. The contributions of naphthalene moieties to the remaining spectral features are largely of σ character. It should also be accounted for the *tert*-butyl contributions in interpreting all those spectra.

To illustrate better the evolution of the features A (HOMO) and B with linear benzo annelation, in Figure 6 photoemission spectra of the valence region onset are shown for thin films of H_2P0, H_2P1, and H_2P2 on an enlarged scale. The photon energy was 75.8 eV. The peak maxima of the HOMO are found at 6.57 ± 0.07, 5.9 ± 0.07, and 5.61 ± 0.07 eV for H_2P0, H_2P1, and H_2P2 films, respectively (compare Table 1). Clearly, the HOMO binding energy decreases for increasing size of the molecular π system. The shifts are in good agreement with theoretical studies,[14,17] suggesting that the linear benzo annelation causes a decrease of the first ionization potential of the molecule. According to ref 14, the b_{1u} orbital is the HOMO−1 for H_2Pc and this b_{1u} orbital in H_2Pc, H_2Nc, and H_2Ac is not influenced by the extension of the macrocycle because it is localized mainly on the nitrogen atoms. We expect a similar behavior for H_2P0, H_2P1, and H_2P2. Therefore, the photoemission signal in the 7 to 9 eV range (band B) is partly attributed to a nonshifting b_{1u}-like orbital of H_2Pc with additional contributions from the benzo units. The latter explains the increased intensity, especially for H_2P1.

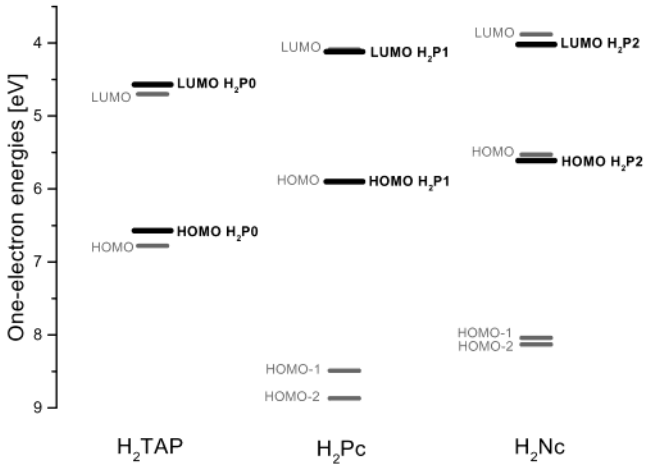

Figure 7. Comparison between the HOMO and the LUMO binding energies as deduced in the present experiments for H_2P0, H_2P1, and H_2P2 and the one-electron energy levels obtained in ref 14 for metal-free tetraazaporphyrin (H_2TAP), metal-free phthalocyanine (H_2Pc), metal-free naphthalocyanine (H_2Nc). The theoretical energy scale was shifted by 0.52 eV to align the theoretical energy of the HOMO for H_2Pc with the experimentally determined binding energy for H_2P1. Thick lines refer to the experimental data whereas thinner lines represent theoretical values.

Binding Energies: Comparison with Theory. The destabilization of the HOMO with linear benzo annelation has been attributed to the antibonding interactions with the fused benzo units.[14] According to the results for unsubstituted compounds,[14] the HOMO is largely localized on the central tetraazaporphyrin (porphyrazine) ring for all those molecules and the antibonding interactions increase with an increasing number of benzo units. The HOMO energy shifts with the addition of each benzo ring. However, the extent of this shift decreases the larger the number of benzo rings, because the interaction of the outer benzo rings with the inner central ring is reduced in comparison to that of the inner ones.[14] Experimentally, we found shifts of 0.67 and 0.29 eV between H_2P0 vs H_2P1 and H_2P1 vs H_2P2, respectively, as summarized in Table 1. The HOMO binding energies in combination with optical absorption data (for the molecules in benzene solution) allow for a rough estimate of the LUMO binding energies via $E_{LUMO} = E_{HOMO} - E_{abs}$ (column 4 in Table 1), where E_{abs} corresponds to the optical absorption energy. Note that this simple approach neglects any solid-state interaction as well as differences due to different final states. Also given in Table 1 are the calculated HOMO and LUMO energies of the respective nonsubstituted molecules as given in ref 14, because no theoretical data for the *tert*-butyl-substituted compounds are available. We recall that no experimental binding energies have been reported for unsubstituted metal-free tetraazaporphyrin (H_2TAP) or its substituted counterpart. However, in addition to the calculations in ref 14, several theoretical studies on the electronic structure of H_2TAP have been performed.[3,13,17,32−34]

Figure 7 summarizes the HOMO and LUMO energies determined experimentally in the present study for H_2P0, H_2P1, and H_2P2 (thick lines), together with the theoretical results of Orti et al.[14] for metal-free tetraazaporphyrin (H_2TAP), metal-free phthalocyanine (H_2Pc), and metal-free naphthalocyanine (H_2Nc), respectively. As the calculated energies generally refer to isolated molecules, the theoretical values from ref 14 entering into Figure 7 were shifted by 0.52 eV toward lower values to align the theoretical HOMO energy for H_2Pc with the experimental binding energy obtained for H_2P1. With this adjustment the overall agreement between the experimental and theoretical energies is good. This indicates that the observed energy shifts

of the HOMO can be explained in a fully molecular picture. Furthermore, it strengthens the argument that *tert*-butyl substitution leads to only minor modifications of the electronic structure of the porphyrazine macrocycle.

Conclusions

On the basis of photoemission measurements using synchrotron radiation, the electronic structure of thin films of benzo-annelated porphyrazine molecules has been studied for three different ligand sizes. The HOMO binding energy decreases with linear benzo-annelation from 6.57 ± 0.07 to 5.90 ± 0.07, and 5.61 ± 0.07 eV for the *tert*-butyl-containing -tetraazaporphyrin, phthalocyanine, and naphthalocyanine compounds, respectively. These shifts are in good agreement with theoretical calculations for structurally similar, but unsubstituted molecules.[14] Indirectly determined LUMO energies, as obtained from optical absorption spectra of the molecules in solution, also agree with the theoretical data. The presence of a *tert*-butyl substituent does not alter the electronic valence structure of the macrocycle significantly as inferred by comparing photoemission data of substituted and unsubstituted molecular films.

References and Notes

(1) Louati, A.; El Meray, M.; André, J. J.; Simon, J.; Kadish, K. M.; Gross, M.; Giraudeau, A. *Inorg. Chem*. **1985**, *24*, 1175.

(2) Hale, P. D.; Pietro, W. J.; Ratner, M. A.; Ellis, D. E.; Marks, T. J. *J. Am. Chem. Soc.* **1987**, *109*, 5943.

(3) Ghosh, A.; Gassman, P. G.; Almlöf, J. *J. Am. Chem. Soc*. **1994**, *116*, 1932.

(4) Nalwa, H. S.; Hanack, M.; Pawlowski, G.; Engel, M. K. *Chem. Phys.* **1999**, *245*, 17.

(5) Reimers, J. R.; Lü, T. X.; Crossley, M. J.; Hush, N. S. *Chem. Phys. Lett.* **1996**, *256*, 353.

(6) Leznoff, C. C.; Lever, A. B. P. *Phthalocyanines. Properties and Applications*; VCH: New York, 1989; Vol. 1.

(7) Leznoff, C. C.; Lever, A. B. P. *Phthalocyanines. Properties and Applications*.; VCH: New York, 1993; Vol. 3.

(8) Tomiyama, T.; Watanabe, I.; Kuwano, A.; Habiro, M.; Takane, N.; Yamada, M. *Appl. Opt.* **1995**, *34*, 8201.

(9) Ali, H.; van Lier, J. E. *Chem. Rev.* **1999**, *99*, 2379.

(10) Nalwa, H. S.; Kakuta, A.; Mukoh, A. *J. Phys. Chem.* **1993**, *97*, 1097.

(11) Hanack, M.; Dürr, K.; Lange, A.; Osío Barcina, J.; Pohmer, J.; Witke, E. *Synth. Met.* **1995**, *71*, 2275.

(12) Carniato, S.; Dufour, G.; Rochet, F.; Roulet, H.; Chaquin, P.; Giessner-Prettre, C. *J. Electron Spectrosc. Relat. Phenom.* **1994**, *67*, 189.

(13) Lamoen, D.; Parrinello, M. *Chem. Phys. Lett.* **1996**, *248*, 309.

(14) Orti, E.; Crespo, R.; Piqueras, M. C.; Tomás, F. *J. Mater. Chem.* **1996**, *6*, 1751.

(15) Nguyen, K. A.; Pachter, R. *J. Chem. Phys.* **2001**, *114*, 10757.

(16) Baerends, E. J.; Ricciardi, G.; Rosa, A.; van Gisbergen, S. J. A. *Coord. Chem. Rev.* **2002**, *230*, 5.

(17) Kobayashi, N.; Konami, H. In *Phthalocyanines. Properties and Applications*; Leznoff, C. C., Lever, A. B. P., Eds.; VCH: New York, 1996; Vol. 4, Chapter 9.

(18) Jerwin, K.; Wasgestian, F. *Spectrochim. Acta, Part A* **1984**, *40A*, 159.

(19) Kovshev, E. I.; Luk'yanets E. A. *Zh. Obshch. Khim*. **1972**, *42*, 696.

(20) Freyer, W. *J. Prakt. Chem*. **1994**, *336*, 690.

(21) Cook, M. J.; Dunn, A. J.; Howe, S. D.; Thomson, A. J. *J. Chem. Soc., Perkin Trans. 1* **1988**, 2453.

(22) Linstead, R. P.; Whalley, M. *J. Chem. Soc.* **1952**, 4839.

(23) Freyer, W.; Minh, L. Q. *Monatsh. Chem*, **1986**, *117*, 475.

(24) Freyer, W.; Stiel, H.; Teuchner, K.; Leupold, D. *J. Photochem. Photobiol. A: Chem.* **1994**, *80*, 161.

(25) Schlettwein, D.; Tada, H.; Mashiko, S. *Thin Solid Films* **1998**, *331*, 117.

(26) Edwards, L.; Gouterman, M. *J. Mol. Spectrosc.* **1970**, *33*, 292.

(27) Gatzke, J.; Winter, B.; Quast, T.; Hertel, I. V. *Proc. SPIE* **1998**, *3464*, 14.

(28) Orti, E.; Brédas, J.-L. *J. Am. Chem. Soc*. **1992**, *114*, 8669.

(29) Orti, E.; Brédas, J.-L. *J. Chem. Phys.* **1988**, *89*, 1009.

(30) Orti, E.; Crespo, R.; Piqueras, M. C.; Viruela, P. M.; Tomás, F. *Synth. Met.* **1993**, *55*−*57*, 4513.

(31) Orti, E.; Piqueras, M. C.; Crespo, R.; Tomás, F. *Mol. Cryst. Liq. Cryst. A* **1993**, *234*, 241.

(32) Toyota, K.; Hasegawa, J.; Nakatsuji, H. *Chem. Phys. Lett.* **1996**, *250*, 437.

(33) Ghosh, A.; Vangberg, T. *Theor. Chem. Acc.* **1997**, *97*, 143.

(34) Miwa, H.; Makarova, E. A.; Ishii, K.; Luk'yanets, E. A.; Kobayashi, N. *Chem. Eur. J.* **2002**, *8*, 1082.